

Catalyst Layer Ink Interactions That Affect Coatability

Marm B. Dixit, 1,* Brice A. Harkey, Fengyu Shen, 1,2 and Kelsey B. Hatzell 6,2,3,**,z

- ¹Department of Mechanical Engineering, Vanderbilt University, Nashville, Tennessee 37240, USA
- ²Interdisciplinary Department of Material Science, Vanderbilt University, Nashville, Tennessee 37240, USA
- ³Department of Chemical and Biomolecular Engineering, Vanderbilt University, Nashville, Tennessee 37240, USA

Catalyst layer inks are examples of biphasic material systems composed of a solid material, a polymer, and a solvent. Nanoscale interactions between the individual constituents can alter macroscopic properties that are relevant for coating and manufacturing processes (i.e. viscosity, surface tension, aggregation, and rheology). Control over these macroscale properties are important for controlled electrode formation during scalable roll-to-roll manufacturing. The underlying interactions include polymer|particle, particle|solvent, and polymer|solvent interactions. In this work we systematically investigate polymer|particle interactions via studying a range of formulated inks composed of different solvents (methanol, isopropyl alcohol, octanol, and water), varying polymer loadings, and particles with different surface charges. Ink aging is also addressed and over short time periods (<1 hr shelf life) the addition of a perfluorosulfonic acid ionomer was shown to stabilize the ink and also decrease the aggregation size. However, over long time periods (168 hrs) the aggregation size is independent of polymer loading, and approaches a steady state aggregation size around 350 nm. This equilibrium point suggests that the polymer is free to diffuse, adsorb, and relax within the excluded volume region. Furthermore, these results suggest that primary aggregates can be broken up with the addition of very low polymer loadings (15% I:C). A semi-empirical model is used to describe polymer|particle interactions within the ink, and the polymer coverage at the surface of the carbon was found to be the most sensitive parameter dictating ink stability. Finally, coating and rheology experiments are completed on all inks.

© The Author(s) 2018. Published by ECS. This is an open access article distributed under the terms of the Creative Commons Attribution 4.0 License (CC BY, http://creativecommons.org/licenses/by/4.0/), which permits unrestricted reuse of the work in any medium, provided the original work is properly cited. [DOI: 10.1149/2.0191805jes] (cc) BY

Manuscript submitted January 4, 2018; revised manuscript received March 2, 2018. Published March 16, 2018. This was Paper 1389 presented at the National Harbor, Maryland Meeting of the Society, October 1–5, 2017.

Scalable manufacturing of catalyst layers and membrane electrode assemblies (MEA) represents an important challenge limiting the adoption of polymer electrolyte fuel cells (PEFC). A MEA is comprised of a proton conducting polymer membrane sandwiched between two catalyst layers and can be considered a multilayer coating. Typically, solution processed techniques that can be readily integrated into roll-to-roll coating lines have been explored for manufacturing (i.e. spray coating, doctor blade, slot-die). 1,2 These methods require processing the active material (carbon, ionomer, and catalyst) in a solvent (Fig. 1a). Recent work on tailoring and designing the feedstock material or ink has mainly focused on tuning the viscosity and surface tension of the ink and surface properties of the substrate. These objectives can be accomplished via altering the constituent loading (solid content) in an ink or changing the solvent.^{3–10} This approach is sound for non-active coatings such as paints and barrier coatings but has significant drawbacks for active coatings (i.e. electrodes). Unlike inactive coatings, catalyst layer coatings are active and need to promote ion, electron, and gas transport. 11 The underlying microstructure and material arrangement within the catalyst layer is critical for promoting efficient mass transport, good catalytic activity, and high adhesion properties. 11,12

Nano-scale interactions within an ink (polymer | particle, particle | solvent, and polymer| solvent) govern macro-scale properties such as rheology, ink stability, and coatability (Fig. 1b). Thus, the ability to control and tune these interactions may provide a means for controlling the catalyst layer microstructure during shear-processing. Significant attention has been focused on understanding how perfluorosulfonic ionomer (PFSI) interacts in different solvent systems because of its complex structure. 13,14 PFSA is characterized by a hydrophobic backbone and a hydrophilic side chain and does not form a true solution but instead has the tendency to form a colloid structure when dispersed in a solvent. Uchida et al. demonstrated that PFSA properties were fundamentally a function of the solvents dielectric constant. In an organic solvent PFSA formed a solution (ε >10), colloid ($3<\varepsilon<$ 10), and a precipitate $(\varepsilon < 3)$.⁴ Shin et al. demonstrated that this colloid structure could be exploited to control the porosity of a catalyst layer.¹⁵ Specifically larger pores were achieved with inks composed of PFSA

in a colloid form as compared with PFSA in a solution form. The main chain mobility of the perflurosulfonic ionomer within the solvent was also shown to have a large impact on the catalyst layer electrode formation. PFSI with high main chain (Polytetrafluoroethylene, PTFE) mobility demonstrated a dense and fine catalyst microstructure, and solvents that promoted high main and side chain mobility formed catalyst layers with greater electrochemical properties. ¹⁶ Emerging challenges with the use of PFSI in the catalyst layer is the propensity for the sulfonic acid side chain to block catalyst active sites resulting in decreased activity and ionomer densification which limits O₂ transport. ^{17,18} The ability to control the interactions between the constituent species within an ink phase may provide an avenue for microstructural control. Furthermore, there is a growing need for understanding how shear-based manufacturing processes and solvent removal stages affect the formation of the microstructure.

Fundamentally, inks are heterogeneous biphasic material systems and are governed by a suite of dynamics across numerous time and length scales. This paper specifically focuses on understanding how these fundamental interactions affect process-related properties and coating processes. We systematically demonstrate how polymer loading, particle surface chemistry, ink formulation, and ink age affect properties related to aggregation and sedimentation. Moreover, we qualitatively compare Derjaguin, Landau, Verwey, and Overbeek theories with an extended approach to provide insight into the complex underlying interactions within an ink. Finally, we evaluate substrate effects through a coating experiment on gas diffusion media with and without a microporous layer, which highlights the importance of formulation and the solvent removal stage on achieving uniform coatings. Prior studies have emphasized the importance of single material system properties such as solvent dielectric constant or polymer loading for effective ink formulation. Herein, we seek to focus on the importance of polymer|particle interactions on electrode formation.

Experimental Methods

Materials and ink formulation.—Vulcan Carbon (VC) XC-72 (Fuel Cell Store, USA) was used as the solid material and solvents were all reagent grade from Fisher Scientific (Table I). Nafion D521 (Fuel Cell Store, USA) dispersion was used as the ionomer for all formulated inks. Low loaded inks (0.1 wt%) were studied for sedimentation and were formulated with ionomer:carbon ratios (I:C) of

^{*}Electrochemical Society Student Member.

^{**}Electrochemical Society Member.

^zE-mail: Kelsey.B.Hatzell@Vanderbilt.edu

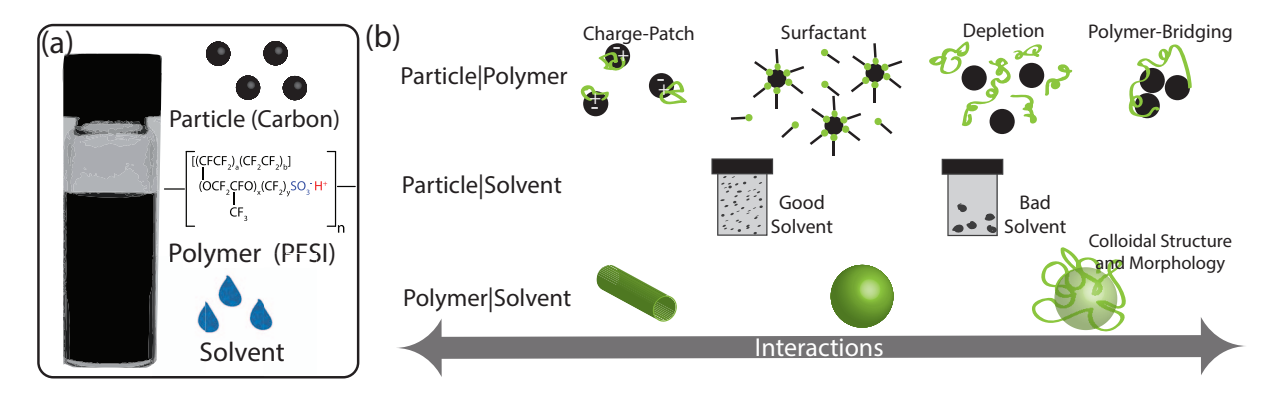


Figure 1. Catalyst layer inks are examples of multicomponent dispersions which contain perflurosulfonic acid, a carbon based material, and a solvent (a). This complex colloidal system has several governing local interactions that can affect coatability and electrode formation during processing and manufacturing (b).

15, 30 and 50. The mass loading of ionomer was calculated by:

$$W_{ionomer} = \frac{m_{ionomer}}{m_{ionomer} + m_{carbon}} * 100$$
 [1]

All inks were mixed with an ultrasonic probe for 10 minutes (1 min on, 1 min off) to homogenize the ink. Visual studies were performed on inks (0.1 wt%) to observe sedimentation. A mild oxidation process where VC was mixed in 1 M $\rm H_2SO_4$ for 1 hour was employed to change the surface functionality of the carbon. Oxidized samples were washed with excessive deionized water and dried in a vacuum furnace. Inks used in coating and rheology experiments were loaded with 10 wt% VC and Nafion. Inks coated on gas diffusion layers were prepared by ball-milling the constituents in methanol for 1 hour at 500 rpm in a planetary ball mill (Pulverisette 7, Fritsch Co.).

Ink characterization.—Dynamic Light Scattering measurements were conducted on a Malvern Nano-ZS Zetasizer instrument in order to assess aggregation and agglomeration in each ink. The physical properties of the solvents used in this study is represented in Table I and the refractive index of carbon was taken as 2.41. Dynamic surface tensions measurements of the carbon inks were measured with a Kruss BP-50 tensiometer. Surface tensions were recorded for bubble ages from 15 ms to 10000 ms at approximately 22°C. Absorbance spectra of undiluted inks were obtained in the range of 800–200 nm using a Varian Cary 5000 spectrophotometer. The absorbance of the first visible peak (\approx 313 nm) was used for comparison and evaluating dispersability of all inks. All particle size, surface tension, and absorbance measurements were completed on inks that were ultrasonically mixed for 20 minutes.

Rheological measurements.—Inks used in coating experiments were rheologically studied using a DHR3 Hybrid Rheometer (TA instruments, USA). All inks were studied using a parallel plate geometry with 1000 μ m gap thickness. All inks were presheared at 100 s⁻¹ for 10 s and allowed to rest for 15 minutes prior to any tests to remove any mechanical history in the samples. Shear sweeps were run from 200 s⁻¹ to 0.01 s⁻¹. Frequency sweeps were run from 0.1 rad/s to

 $\label{thm:continuous} \textbf{Table I. Solvents proposed to be used in this study with key physical properties.}$

Key	Solvent	Viscosity [cP]	Dielectric Constant[-]	Surface Tension[mN/m]
A	Water	1	80.1	72.8
В	Iso Propyl Alcohol	2.04	19.92	21.7
C	Methanol	0.56	32.7	22.2
D	Glycerol	1412	42	63.0
E	1-octanol	7.363	10.3	27.5

600 rad/s. A constant amplitude of 0.1% was applied during oscillating experiments.

Ink processing and characterization.—An automatic film coater (MTI Corporation) was used for coating experiments. Two substrates were examined as substrates for the carbon inks: Sigracet 29AA, and Sigracet 29BC (Fuel Cell Store). Each substrate was stabilized prior to coating with a vacuum baseplate. All coating experiments were conducted at a gap width of 350 μm and coating speed of 15 mm/s. Scanning electron microscopy (5 keV, HE-SE2 detector) images were obtained on a Zeiss Merlin SEM.

Aggregation Model

A catalyst layer ink is an example of a complex material system comprised of a solid material, a polymer, and a solvent. Due to the length scale of the solid carbon material (<50 nm), these inks can be considered polymer/colloid systems.²⁰ There is an immense body of literature which reports polymer/colloid systems for self-assembly applications,²¹ composite materials processing,²² and nano-materials synthesis.²³ In all of these systems there is interest in tuning the underlying interactions for either controlled structural or physical properties. The interactions between the polymer and colloid are namely van der Waals, electrostatic repulsion, steric/depletion, hydration, and hydrodynamic interactions. To understand the aggregation, flocculation, and sedimentation dynamics in these ink-like systems Derjaguin, Landau, Verwey, and Overbeek (DLVO) theories have been employed with population balance models.²⁴ This simplified model assumes van der Waals interactions and coulombic forces are the dominating dynamics within an ink (Fig. 3a):

$$U_{vdW} = -\frac{A}{6} \frac{a_i a_j}{(a_i + a_j)} \frac{1}{r - (a_i + a_j)}$$
[2]

$$U_{cf} = \frac{4\pi\epsilon_m^*\psi^2(a_i + a_j)^2}{r}$$
 [3]

where, A is the Hamaker constant, ai is the particle radius, r is the interparticle distance, ϵ_m^* is the electric permittivity of the medium, and ψ is the zeta potential of the colloidal system. The Hamaker constant can be estimated using the following expression:

$$A = \frac{3}{4}k_B T \left(\frac{\epsilon_p - \epsilon_m}{\epsilon_p + \epsilon_m}\right)^2 + \frac{3h\nu_e}{16\sqrt{2}} \frac{\left(n_p^2 - n_m^2\right)^2}{\left(n_p^2 + n_m^2\right)^{3/2}}$$
[4]

Formulations of these interactions have been well-studied and the physical parameters necessary to parameterize them are readily available or quantifiable.³ It should be noted that the coulombic interaction may not be sufficient in describing the electrostatic interaction in aqueous inks. This is because the physical properties of water can

change near hydrophobic surfaces (i.e. carbon black) and ultimately lead to an over-prediction of the ink stability.²⁵

Phenomenologically the classical DLVO theory neglects any interaction which may come into play with the addition of a polymer. Polymer behavior is dictated by the nature of the colloidal system and the particle|polymer interaction. While polymer systems can be described as an ionic solution with electrostatic effects, the major difference between them lies in the internal degrees of freedom of the polymer. Thus, an accurate description of the polymer|particle interaction requires an in-depth consideration of the thermodynamics of the polymer solutions. Scaling theory is used to calculate the force acting due to an adsorbed polymer layer via minimization of a surface free energy function subject to a constant polymer coverage constraint. This theory is generally preferred due to the limited number of parameters needed to define the interaction. Furthermore, these parameters can be theoretically obtained from experiments. The surface energy function according to this theory is:

$$\gamma - \gamma_0 = -|\gamma_1| \Phi_S + \alpha_{Sc} k_B T * \int_0^r \frac{1}{\xi^3(\Phi)} \left[1 + \left(\frac{\xi(\Phi)}{\Phi} \frac{d\Phi}{dz} \right)^2 \right] dz$$

where γ and γ_0 are the surface free energy of the polymer solution and the solvent, k_b is the Stefan - Boltzmann Constant, T is the temperature, $\Phi(z)$ is the polymer concentration as a function of distance from the surface with Φ_s as the limiting value at the surface. The local polymer-interface interaction energy per unit area (γ_1) has a negative value for adsorbing surfaces and α_{Sc} and m_0 are constants.²⁸ The local correlation length that depicts the average distance between consecutive contact points of a polymer chain with other chains is given as $\zeta(\Phi)$. The first term on the right hand side of Equation 5 accounts for the short-range surface contribution while the second term depicts the bulk contribution to the surface energy. The shortterm interaction is mainly dependent on the polymer concentration at the surface, while the latter consists of an entropic term as well as an excluded volume interaction. The first term inside the integrand accounts for the local interaction density due to to polymer segments, while the second term depicts the entropic cost of maintaining a non-uniform segment composition profile within the adsorbed layer. When two polymer covered surfaces are brought close to each other, it is expected that a symmetric polymer concentration profile will develop between the surface with a maximum value at the surface that decays to a minimum bulk value at the midpoint between the surfaces. However, it was observed that at very short separations, the polymer concentration profile between the surfaces essentially becomes a constant,²⁹ i.e. $\Phi(z) \approx \Phi_S \approx \Phi_{midpoint} \approx \Gamma a_m^3 r$, where Γ is the total polymer adsorbed on the surface, Φ_S and $\Phi_{midpoint}$ are the polymer concentrations at the surface and midpoint between surfaces respectively, a_m is the effective monomer size, r is the distance of closest approach of the particles. Under this limiting assumption, the surface energy function defined in Equation 5 can be simplified to,

$$\gamma - \gamma_0 = -|\gamma_1| \, \Phi_S + \left(\frac{\alpha_{Sc} k_B T}{a_m^3}\right) r \Phi_{midpoint}^{9/4} \tag{6}$$

Using this equation, the intersurface pressure can be calculated as,

$$\Pi_{d} = -\frac{\partial \left(2\gamma\right)}{\partial \left(2r\right)} \approx \left(\frac{\alpha_{Sc}k_{B}T}{a_{m}^{3}}\right)\Phi_{0}^{\frac{9}{4}} \left[-\frac{32\Gamma}{\omega^{2}\Gamma_{0}} + \frac{5}{4}\left(\frac{8\Gamma}{\omega_{Sc}\Gamma_{0}}\right)^{2}\right]$$
[7]

where, $\omega_{Sc} = 2r/D_{Sc}$ is the reduced length, $\frac{\Gamma}{\Gamma_0}$ is the fractional coverage of the surface compared to saturated coverage, Φ_0 is the polymer concentration at a single saturated surface, and D_{Sc} is a characteristic scaling length. The scaling length and saturation polymer concentration can be obtained by scattering and reflectivity experiments.³⁰ Integrating the equation for intersurface pressure yields the interaction

energy between flat surfaces.

$$U_{polymer}^{plate} = \left(\frac{\alpha_{Sc}k_{B}T}{a_{m}^{3}}\right)\Phi_{0}^{\frac{9}{4}}D_{Sc}\left[-\frac{16\Gamma D_{Sc}}{r^{2}\Gamma_{0}} + \frac{D_{Sc}^{5/4}}{(2r)^{5/4}}\left(\frac{8\Gamma}{\Gamma_{0}}\right)^{9/4}\right]$$
[8]

Applying the Derjaguin approximation³¹ to this formulation yields the interaction energy for two equal, polymer coated spheres. Further, applying the relationship proposed by Napper,³² interaction energy between two unequal polymer coated spheres can be expressed as,:³⁰

$$U_{poly}(r) = \pi * a_i \left(\frac{\alpha_{Sc} k_B T}{a_m^3} \right) \Phi_0^{\frac{9}{4}} D_{Sc}$$

$$\times \left[-\frac{16\Gamma D_{Sc}}{\Gamma_0} \ln \left(\frac{2\delta}{r} \right) + \frac{4D_{Sc}^{\frac{5}{4}}}{2^{\frac{5}{4}}} \left(\frac{8\Gamma}{\Gamma_0} \right)^{\frac{9}{4}} \left(\left(\frac{1}{r} \right)^{\frac{1}{4}} - \left(\frac{1}{2\delta} \right)^{\frac{1}{4}} \right) \right]$$
[9]

 a_i is the primary particle radius, δ is the thickness of adsorbed polymer. It should be noted that the set of parameters inside the first brackets represent a scaling force term that can be experimentally determined by surface force balance measurements. The first term in the square brackets represent the short range attraction, while the second term represents the repulsion due to excluded volume. Relative magnitude of these terms determine whether polymer adsorption results in steric repulsion or bridging attraction.

The total interaction energy is given by:

$$U_{tot}(r) = U_{vdW} + U_{cf} + U_{poly}$$
 [10]

The collision efficiency α can be estimated as the inverse of the stability ratio, which is given as follows:

$$W = \frac{1}{\alpha} = (a_i + a_j) \int_{a_i + a_j + a_{thres}}^{\infty} \frac{1}{r^2} \exp\left(\frac{U_{tot}(r)}{8k_B T}\right) dr$$
[11]

Assuming perikinetic aggregation, the population balance equation for the particle k forming from the collision of particle i and j, can be written as.

$$\frac{dn_k}{dt} = \alpha \left(\frac{K_{ij}}{2} \sum_{i=1; j=k-i}^{i=k-1} n_i n_j - K_{ij} n_k \sum_{i=1}^{\infty} n_i \right)$$
 [12]

where n_i , n_j and n_k are the particle concentrations of aggregates i, j and k respectively, and K_{ij} , is the aggregation rate constant which is given as,

$$K_{ij} = \frac{8k_b T}{3\mu} \frac{\left(a_i + a_j\right)^2}{a_i a_i}$$
 [13]

The threshold settling size is assumed to be 450 nm $(n_t/n_0 = 0.00053)$. In this model a monodispersed system was assumed and the settling time was computed using a modified population balance equation: ^{33,34}

$$\frac{dn_t}{dt} = -\alpha \frac{K_{ij}}{2} n_t^2$$
 [14]

The aggregation rate, in the initial time where particle size can be considered constant can be given as,

$$K_{ij} = \frac{8k_b T}{3\mu} \tag{15}$$

The parameters used in the simulations are listed in Table II. The refractive index and dielectric constant for the carbon was taken as 1.8 and 2.5, respectively.³ The primary particle size was considered to be 50 nm, as specified by the supplier.

Results and Discussion

Ink stability, aging, and formulation are important considerations for quality control and manufacturing of catalyst layers. There are numerous interactions within an ink (polymer|solvent, solvent|particle,

Table II. Physical properties used in the DLVO and XDLVO model.

Zeta Potential (mV)	a_m (nm)	δ (nm)	Ψ_0
29.4 [35]	25 [46]	20	0.5 [47]
-71.1[35]	17 [14]	30 [48]	0.35
-28.5[35]	25 [49]	15	0.44 [47]
-44.9[3]	20 [49]	15 [50]	0.44
-2.7[3]	N.A.	N.A.	N.A.
	Potential (mV) 29.4 [35] -71.1 [35] -28.5 [35] -44.9 [3]	Potential (mV) a_m (nm) 29.4 [35] 25 [46] -71.1 [35] 17 [14] -28.5 [35] 25 [49] -44.9 [3] 20 [49]	Potential (mV) a_m (nm) δ (nm) 29.4 [35] 25 [46] 20 -71.1 [35] 17 [14] 30 [48] -28.5 [35] 25 [49] 15 -44.9 [3] 20 [49] 15 [50]

and polymer|particle) that govern aggregation and sedimentation properties. Both of these phenomena can play a significant role in the formation of the electrode microstructure in terms of the packing density, polymer distribution and placement, and processability. Figure 2a shows a visual aging study for Vulcan carbon dispersions in different solvents at zero days and after a shelf-life of 15 days. The solvent strongly determines the dispersability of an ink when the ink does not have a polymer (Fig. 2a samples A-E), yet plays a limited role when the ink contains a polymer (Fig. 2a samples C1-C3). Carbon inks based in methanol (1 hr) and octanol (30–43 hr) are highly unstable and sediment faster than inks based in water, IPA, and glycerol. The VC dispersions in water, IPA, and glycerol were stable ≥3 months. Carbon particles within an ink are subjected to electrostatic repulsions and van der Waals forces. The magnitude of the former interaction

can be estimated from the zeta potential and decreases in the order: Water>Methanol>IPA.³⁵ The zeta potential for octanol and glycerol can be estimated from the dielectric constant and it can be assumed that glycerol would fall between water and methanol, and octanol would have the lowest zeta potential. The relative strength of van der Waals attraction can be estimated by the Hamaker's constant³⁶ which decreases as: Water>Methanol>IPA>Octanol>Glycerol. Methanol dispersions are dominated by strong attractive interactions which leads to rapid sedimentation. Octanol on the other hand has weak attractive and repulsive interactions which may describe the delayed sedimentation observed in the experiments (Fig. 2a).

Understanding how the cohesion energy of a solvent is related to individual solvent solubility parameters is important for tailoring a dispersion's stability via solvent design. The Hildebrand solubility coefficient (δ_T) is fundamentally related to the square root of the cohesive energy and can be described by:

$$\delta_T = \sqrt{\frac{\Delta H \nu - RT}{V_m}}$$
 [16]

where ΔH , ν , R, and T represent the heat of vaporization, gas constant, temperature, and molar volume of the condensed phase. This relationship can be related to the h-bonding (δ_H) , dispersive (δ_D) , and polar (δ_P) bonding hansen parameters as:

$$\delta_T^2 = \delta_D^2 + \delta_H^2 + \delta_P^2$$
 [17]

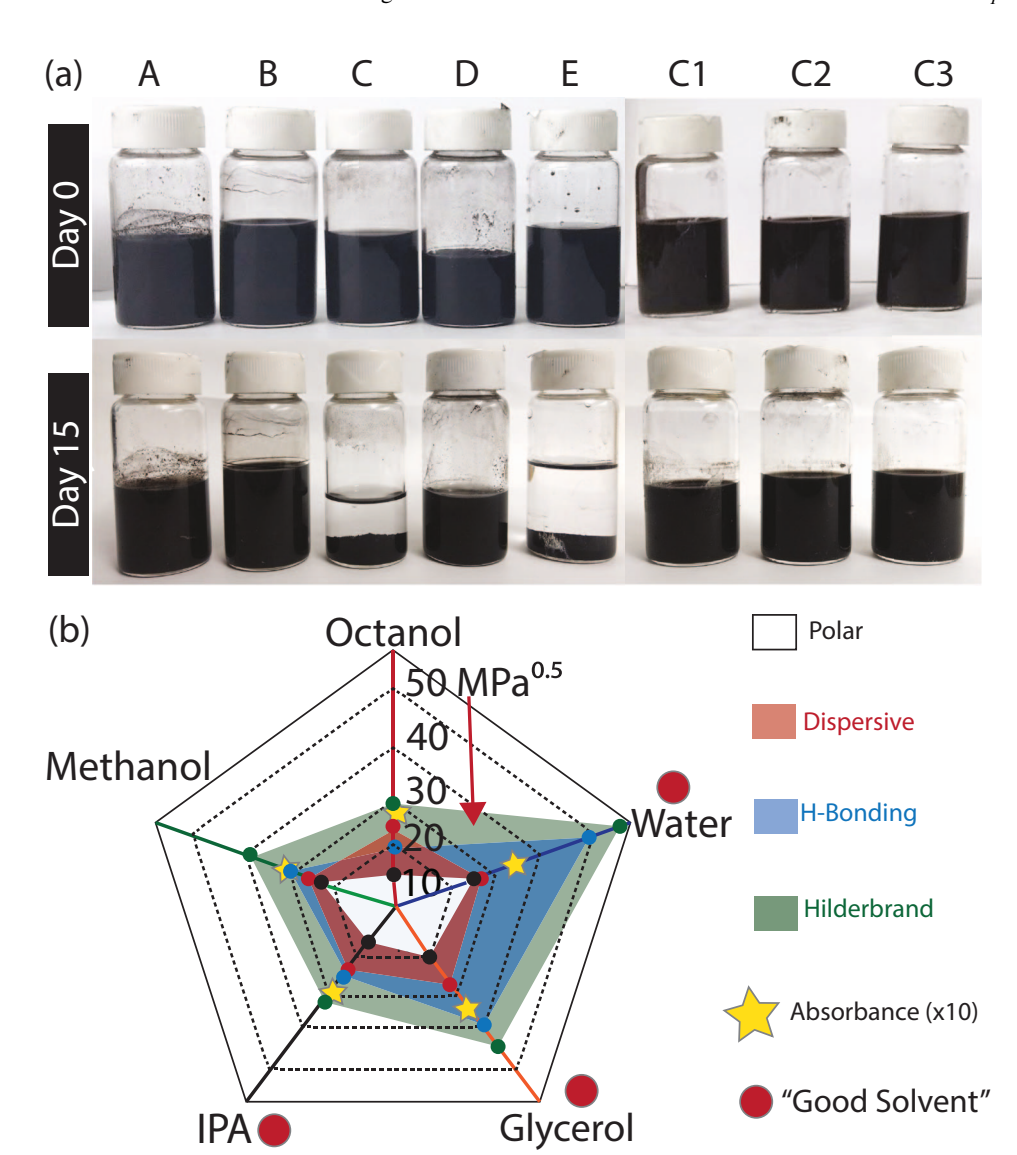


Figure 2. (a) Visual stability analysis. Solvent key as listed in Table I. The sedimentation times for ink C is 1 hour while for ink E is 43 hours. The C1, C2, C3 inks are ionomer containing inks with methanol solvent and I:C ratios of 15, 30 and 50 (b) solvent solubility parameters and absorbance study results.

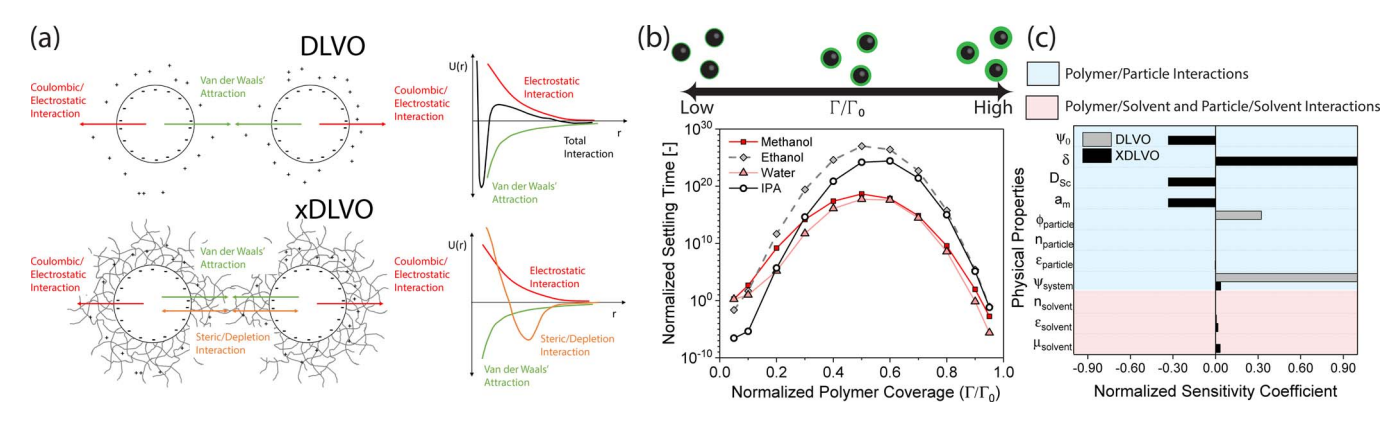


Figure 3. Results from aggregation modeling studies and schematic diagram of interactions in the DLVO and xDLVO models (a). The aggregates normalized settling time in various solvents (b) and a sensitivity analysis for the DLVO and XDLVO model (c). $\frac{\Gamma}{\Gamma_0}$ is the fractional coverage of the surface compared to saturated coverage, μ is the viscosity, ϵ is the dielectric constant, n is the refractive index, Ψ_{system} is the system zeta potential, $\Phi_{particle}$ is the particle porosity, δ is the thickness of adsorbed polymer, a_m is the effective monomer size, Φ_0 is the polymer concentration at a single saturated surface, and D_{Sc} is a characteristic scaling length.

Figure 1b shows a radar plot of the solubility parameters for each solvents plotted with respect to their hilderbrand paramater and absorbance value. Plotting the absorbance value of the investigated ink systems with the Hildebrand parameter shows a peak at \sim 40 MPA $^{1/2}$, suggesting that VC dispersions may be stable in solvents with similar Hildebrand solubility parameters. The magnitude of each solubility parameter (δ_H , δ_T , and δ_P) can be compared with the measured absorbance in order to draw correlations between individual solvent interactions and dispersability. There is a mild correlation between the H-bonding and dispersive parameters and the absorbance peak. These results suggest that solvent selection and design for inks without polymers may be accomplished via tailoring these interactions to absorbance values.

The addition of an ionomer or polymer to the system shows a pronounced effect on the stability and dispersability of an ink system (Fig. 1a). The unstable methanol based ink is seen to be stable for over 3 months duration in the presence of an ionomer. Shukla et al. modeled the effect of ionomer addition as a change in the zeta potential.³ This was rationalized by increasing ion concentration in the inks due to addition of the $-SO_3H$ side chain and was found to be pronounced for solvents with higher dielectric constants. However, apart from electrostatic stabilization, polymer|particle interaction can also have an entropic or osmotic contribution. Previous studies have shown that Nafion has a high equilibrium adsorption coefficient for VC suggesting a strong binding³⁷ and the presence of non-adsorbed polymer in the ink can lead to depletion interactions (Fig. 1b). Particles in inks systems (without a polymer) can aggregate because van der Waals forces are very strong at small separation distances. However, in presence of an adsorbed polymer, the entropic repulsion keeps individual particles from getting close and hence the total interaction acting on the particle system is essentially repulsive leading to a stabilized ink system (Fig. 2a).

Figure 3b demonstrates the normalized settling time for different inks where the normalized settling time is the ratio between the predicted settling time observed with the xDLVO model and DLVO model. While the results have exaggerated values for settling times, they imply that the inks are stable over the expected lifetime of these systems when the ink contains a polymer. These estimates are qualitatively in agreement with our experimental observations on sedimentation and stability. It is observed that the settling times increases by several orders of magnitude with small polymer coverages (Fig. 3b). Each solvent demonstrates a similar profile where stability can be optimized up to a point and then decreases in stability as the polymer coverage is increased. It is unlikely that polymer bridging dynamics (Fig. 1b) occur in catalyst layer inks because sedimentation would happen on the order of seconds rather than minutes, hours, or days. However, as the excluded volume of the inks becomes saturated

with polymer, bridging can be potentially induced. This is observed in the decrease in stability at high polymer coverage. These results suggest that solvent|polymer interactions are weak in comparison to the polymer|particle interactions.

DLVO and xDLVO formulations show vastly different sensitivity parameters because of the varying interactions. The most sensitive parameter in the DLVO model is the zeta potential (ψ_{system}) which suggests that the electrostatic repulsion is the dominant force in this formulation. Experimentally this is obviated via a comparison between the particle size of a polymer-free ink composed of VC and oxidized VC. It is widely understood that oxidizing carbon decreases the surface charge (more negative) and can thus increase the repulsion dynamics. Table III demonstrates how this increase in repulsion dynamics leads to smaller aggregation size and more stable systems. The inks composed of oxidized carbon are less affected by particle|solvent interactions than the inks composed of bare carbon and demonstrate a narrower range of aggregation sizes ($\approx 250-350$ nm). In contrast, the nonoxidized carbon inks without polymer (Table III) are extremely sensitive to solvent type and the aggregation size varies between 300 and 1000 nm.

For the xDLVO model, the adsorbed polymer layer thickness is the most sensitive parameter and the particle zeta potential and porosity are less sensitive. The latter observation suggests that the polymer interactions dominate in these systems (Fig. 3c). There are challenges in validating the proposed models given the observed exaggerated results. Furthermore, ionomer containing inks are seen to be stable over extended durations (\approx 3 months), making quantitative measurements of sedimentation difficult. There are several limiting assumptions in the population balance model: perikinetic aggregation mode, monodispersed spherical particles, two-body interactions, among others. While these shortcomings restrict the use of the models as quantitative tools, they still can be used as a qualitative tool for prediction of stability of unknown ink systems and describe the underlying physics governing the stability.

Aside from ink stability, ink aging or shelf-life behavior, is another parameter of interest for scalable manufacturing processes. To

Table III. Dynamic Light Scattering reveals the aggregation properties of $0.1~\rm wt\%$ inks with different surface functionalities and no aging.

Solvent	I:C	VC (nm)	VC Ox.(nm)
Water	0	299.07	259.25
Isopropyl Alcohol	0	322.38	237.15
1-Octanol	0	812.09	264.99
Methanol	0	662.34	380.78

Table IV. Dynamic Light Scattering reveals the aggregation properties of 0.1 wt% inks with different surface functionalities, I:C ratios, and aging.

Solvent	I:C	Age (hrs)	VC (nm)[P.D.I.]
Methanol	15	0	554.91 [0.27]
Methanol	30	0	483.65 [0.36]
Methanol	50	0	493.16 [0.34]
Methanol	15	168	366.45 [0.20]
Methanol	30	168	367.26 [0.23]
Methanol	50	168	336.44 [0.18]
Methanol	0	0.16	662.34 [0.29]
Methanol	0	0.66	3240.44 [0.34]
Methanol	0	24	85.22 [0.79]

study the effect of aging on particle size, dynamic light scattering experiments were completed on methanol inks containing 0.1 wt% carbon in methanol immediately after sonicating and after a shelf life of 168 hours. The addition of an ionomer to the ink caused a decrease in aggregation size from 662 nm (0 I:C) to 493 nm (50 I:C) which was similarly shown previously.3 This decrease in aggregation size is potentially due to break up of primary carbon agglomerates as the polymer adsorbs to the particle. After aging, the ionomer containing inks converge to a uniform size which is independent of I:C ratio and very close to stable dispersions obtained from IPA and water (\approx 300–360 nm). The polydispersity index (PDI) is a good indicator of ink stability and will be high (>0.3–0.4) for unstable colloidal systems. Table IV shows that the PDI decreases with the addition of an ionomer and also decreases over a shelf life of 168 hours. This suggest that there a time domain for which the polymer diffuses, adsorbs, and relaxes within the carbon matrix before reaching an equilibrium structure. This time domain is important because it breaks up primary aggregates and further suggests that the fundamental ink structure is independent of solvent. Nevertheless, inks without a polymer are largely dependent on the solvent properties which is apparent by the increasing PDI with time (24 h) for the methanol inks (Table IV). These trends reflect the sedimentation phenomenon occurring in the methanol inks in absence of polymer.

The decrease in particle size with ionomer loading and increased stability of the carbon inks suggests that the ionomer (PFSI) acts like a surfactant. Dynamic surface tension measurements are useful for understanding dynamic processes that involve a large change in area in a short time, typically seen in coating applications (spray, blade coating, etc.). Ideally, dynamic surface tension should be minimized to promote wettability of the ink and should remain constant over time to ensure a defect free coating. When inks are subject to a sudden change in area as experienced during spray coating, it can lead to diffusion of constituents to the free interface to balance the free energy of the coating. This can lead to a non-uniform deposition of active material, and defects like Benard cells, craters, and delamination.³⁸ Thus, dynamic surface tension measurements enable understanding how stable the air liquid interface is for effective coatings. Figure 4a demonstrates the surface tension as a function of surface age for low concentration ink (0.1 wt%) without a polymer in different solvents. Pure solvents show very little variation in dynamic surface tension over time but the addition of VC leads to an increase in the surface tension for all the solvents tested (Fig. 4a). This increase is possibly due to the structuring of the solvent around the dispersed VC particles. Water, which has a very strong structuring effect due to a higher H-bonding interaction, thus shows the highest increase in surface tension on addition of VC. For the ionomer containing inks (Fig. 4b), it is seen that increasing ionomer content as well as increasing the carbon content increases the initial surface tension. A decay is observed in all responses and is subsequently minimized as the ionomer concentration is increased and the stabilization time is reduced. This effect becomes more pronounced as the mass loading is increased (Fig. 4b). Although the ink composed of 2.5 wt% (100 I:C) has the highest initial surface tension it rapidly decays at 100 ms and reaches a similar surface

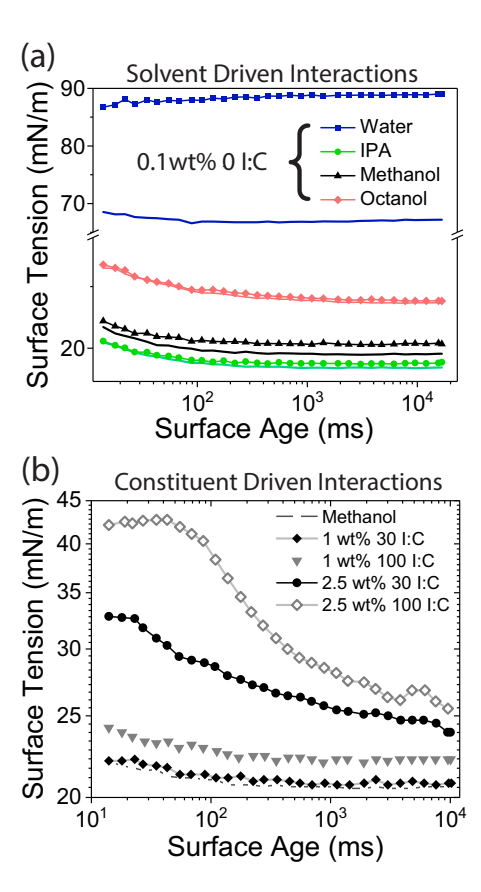


Figure 4. DST measurements of ink systems (a) 0.1 wt% VC ink dispersions in different solvents. Bare solvents are shown by lines, while VC inks are depicted with markers (b). DST measurements for 30 I:C and 100 I:C inks with different formulations.

tension to the 30 I:C samples (\approx 25 mN/m). Samples with greater than 2.5 wt% loading could not be measured because of measurement instabilities but similar trends.

The addition of an amphiphilic polymer to a solution will typically decrease the surface tension.³⁹ However, in catalyst layer hybrid inks containing hydrophobic carbon nanomaterials and PFSI, an increase in surface tension is observed with increasing polymer and solid constituent loading. These results suggest that during coating applications the hydrophobic carbon and polymer may diffuse to the air vapor interface. Furthermore, it is expected that polymer is adsorbed by the carbon leading to an increase in free energy and reduction in the entropy of the system. This can be justified as polymer addition to a colloidal system leads to the following phenomena:⁴⁰ a) change in combinatorial entropy and free energy of the system as the polymer and solvent redistribute themselves between the surface and bulk phases in response to the adsorptive forces of the surface, b) the free energy associated with the interaction of the surface with those solvent molecules and polymer segments which are in actual contact with it, c) the lowering of the entropy of the adsorbed polymer molecules due to restriction on their configurations.

The quality of coated films is dependent on processing parameters, substrate properties, and ink rheology. While processing parameters and substrates can be modified during coating and offer some dynamic control, ink rheology is the limiting parameter that dictates both the manufacturing process (spray coat, doctor blade, slot die, etc.) and manufacturing speed (shear rate) attainable. In order to isolate the effects polymer|particle interactions play in coatings, single solvent inks (10 wt% aqueous) were formulated for a range of I:C ratios. All inks studied demonstrate a shear thinning behavior between 0 and 200 s^{-1} (Fig. 5a). Shear thinning behavior is attributed to formation of layers of aggregates inside the ink phase coincident to the shear

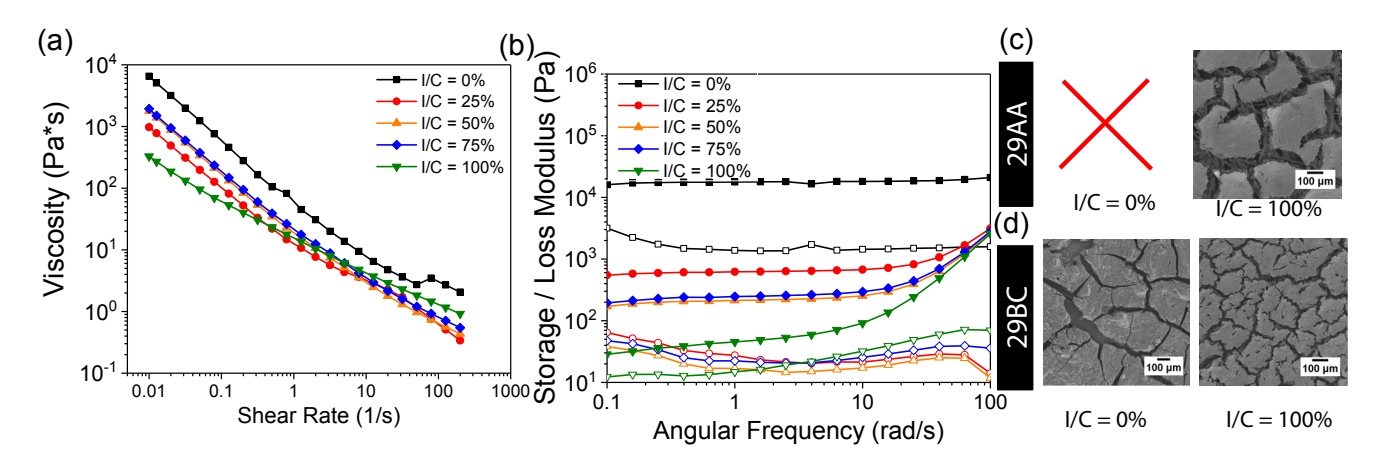


Figure 5. Steady shear sweeps (a) and oscillatory frequency sweeps for 10 wt% VC ink dispersion in water (b). SEM images of coating on Sigracet 29AA substrate. Coatings from 0 I:C inks were unstable and could not be imaged (c) SEM images of coatings on Sigracet 29BC substrate (d).

plane. 42 As the concentration of polymer is increased (I:C ratio) a subsequent decrease in viscosity is observed.⁴³ This decrease in viscosity suggests that the interaction between the polymer and carbon is decreased as the excluded volume region of the ink becomes filled with polymer. The flow behavior and viscosity of the ionomer containing inks are similar and demonstrate a clear dependence on shear rate for steady shear tests. However, notable differences are observed in the oscillatory experiments (Fig. 5b). When there is no polymer in the system (0 I:C) the storage modulus (G') value is highest and independent of angular frequency. Furthermore, the storage is nearly two orders of magnitude larger than the loss moduli indicating the sample resembles gel-like behavior. The storage modulus decreases by three orders of magnitude when the I:C ratio is increased from 0% to 100%. For all the inks, the storage modulus is larger than the loss modulus. This indicates that all inks have a network structure, however the structure becomes increasingly fragile with increasing ionomer content and is visible by an upswing in the loss moduli between 10-100 rad/s. It has been observed that inks with high G' values can lead to hang-up, reduced printing speeds as well as increased loads on the applicator.44

There are two manufacturing approaches typically used for processing catalyst layers: (1) catalyst-coated membrane (CCM) and (2) catalyst coated diffusion-media (CCDM). The former involves the direct application of the catalyst layer onto the membrane via spray approaches or decal transfer methods. There are significant drawbacks with the scalability and level of quality control achieved with these methods because the transfer process is challenging and the membrane swells when exposed to solvents. The latter materials processing approach (CCDM) involves the direct application of the catalyst layer to the gas diffusion electrode. This method benefits from scalability because the gas diffusion electrode can be readily implemented in roll-to-roll lines. However, one drawback is the non-uniform substrate surface which can have significant roughness when coated with a microporous layer (MPL). In order to evaluate the impact of the substrate and ink formulation on coating we chose to study coating our aqueous inks formulated in the rheology experiment onto a substrate without a MPL (Sigracet 29AA) and with a MPL (Sigracet 29BC) (Figs. 5c, 5d). The coatability of the ink depends on its rheology as well as the dynamic surface tension response. While both inks showcase a shear thinning behavior, the power law indexes for both the inks are significantly different. Equivalent power law model for 0 I:C ink response is given as $\mu = 81.265 \,\dot{\gamma}^{0.146}$, while the 100 I:C ink response can be fitted as $\mu = 17.131 \text{ }\dot{\gamma}^{0.414}$. The lower consistency index and higher shear thinning power leads to reduced pressure drops for the 100 I:C ink while coating. This allows for coating of a more uniform layer as compared to 0 I:C ink. The higher storage modulus observed in the 0 I:C ink also restricts the flowability of these inks and can manifest into defects arising from hang-ups at the coater edge. The addition of

the polymer to the ink increases the surface tension and reduces the stabilization time as discussed earlier. The presence of an amphiphilic component allows for proper wetting during coating lower during coating. Furthermore, a lower stabilization time minimizes defects attributed to component diffusion within the coated layer. Substrate effects can also play a role in the quality of the coating obtained. Sigracet 29AA is a carbon paper diffusion media with no PTFE treatment and Sigracet 29BC contains a microporous layer with a 5% PTFE backing. This causes a strong hydrophobic interaction with the inks that can influence the coatings. Stable inks (0 I:C) could not be coated onto the hydrophobic 29AA substrate which could be due to solvent diffusion through the GDL subsequently resulting in nonuniform solvent removal. Consequently, high I:C (100 I:C) inks were able to be coated on the 29AA but with the presence cracks on the order of 100 µm. In contrast, both low and high I:C inks could be coated onto 29BC with crack propagation being significantly reduced at high I:C ratio's. In general, cracking has been observed for water based inks and is attributed to the hydrophobic interactions between the carbon and solvent leading to non-uniform solvent removal processes.⁴⁵ Future work which evaluates crack generation during the solvent removal stage is important for coupling ink design with scalable manufacturing.

Conclusions

Catalyst layers are examples of active coatings that promote proton, electron, and ion transport. There is a tremendous need for microstructural control during manufacturing to enable durable membrane electrodes assemblies with good activity and efficient mass transport. While there has been a significant body of research evaluating fundamental aspects regarding transport and polymer confinement effects within the catalyst layer, there has been far less attention placed on the scalable manufacturing of catalyst layers and the feedstock material or ink. Within a catalyst layer ink there are numerous nano-scale interactions that govern macroscopic processing properties (i.e. viscosity, surface tension, rheology, etc.). These interactions include polymer|solvent, polymer|particle, and particle|solvent interactions. Polymer|particle interactions are important especially in inks with high content loadings which are most notably used in roll-to-roll manufacturing processes that employ blade of slot die methodologies. Herein, we show that these interactions play a significant role in the aggregation properties of inks. Specifically, it is shown that the aggregation size of Vulcan carbon stabilizes to a set value of ≈350 nm after 168 hours and that the aggregation size is independent of polymer loading. To probe the underlying physics the polymer|particle interactions we introduce an extended DLVO model which highlights the importance of polymer coverage on describing aggregation and stability (sedimentation) properties. Future work which can experimentally observe this interaction will be enlightening in terms of promoting controlled interactions within inks.

Acknowledgments

The authors were supported by the National Science Foundation under grant No. 1727863. K.B.H acknowledges support from the Ralph E. Powe Junior Faculty Enhancement Award from ORAU. The authors acknowledge the Vanderbilt Institute of Nanoscience and Engineering (VINSE) for access to their shared characterization facilities.

ORCID

Kelsey B. Hatzell https://orcid.org/0000-0002-5222-7288

References

- K. B. Hatzell, M. B. Dixit, S. A. Berlinger, and A. Z. Weber, *Journal of Materials Chemistry A*, 5, 20527 (2017).
- 2. M. Ulsh, J. M. Porter, D. C. Bittinat, and G. Bender, Fuel Cells, 16, 170 (2016).
- S. Shukla, S. Bhattacharjee, A. Z. Weber, and M. Secanell, *Journal of The Electro-chemical Society*, 164, F600 (2017).
- M. Uchida, Y. Aoyama, N. Eda, and A. Ohta, *Journal of The Electrochemical Society*, 142, 463 (1995).
- M. Chisaka and H. Daiguji, Journal of The Electrochemical Society, 156, B22 (2009).
- D. H. Cho, S. Y. Lee, D. W. Shin, D. S. Hwang, and Y. M. Lee, *Journal of Power Sources*, 258, 272 (2014).
- T. Suzuki, S. Tsushima, and S. Hirai, *International Journal of Hydrogen Energy*, 36, 12361 (2011).
- S. Shukla, K. Domican, K. Karan, S. Bhattacharjee, and M. Secanell, *Electrochimica Acta*. 156, 289 (2015).
- C.-Y. Jung, W.-J. Kim, and S.-C. Yi, International Journal of Hydrogen Energy, 37, 18446 (2012).
- 10. N. Zamel, Journal of Power Sources, 309, 141 (2016).
- 11. S. Holdcroft, Chemistry of materials, 26, 381 (2013).
- T. Soboleva, X. Zhao, K. Malek, Z. Xie, T. Navessin, and S. Holdcroft, ACS applied materials & interfaces, 2, 375 (2010).
- 13. M. Ghelichi, K. Malek, and M. H. Eikerling, Macromolecules, 49, 1479 (2016).
- C. Welch, A. Labouriau, R. Hjelm, B. Orler, C. Johnston, and Y. S. Kim, ACS Macro Letters, 1, 1403 (2012).

- S. J. Shin, J. K. Lee, H. Y. Ha, S. A. Hong, H. S. Chun, and I. H. Oh, *Journal of power sources*, 106, 146 (2002).
- T. H. Kim, J. Y. Yi, C. Y. Jung, E. Jeong, and S. C. Yi, *International Journal of Hydrogen Energy*, 42, 478 (2017).
- R. Subbaraman, D. Strmcnik, V. Stamenkovic, and N. M. Markovic, *The Journal of Physical Chemistry C*, 114, 8414 (2010).
- 18. K. Karan, Current Opinion in Electrochemistry, 5, 27 (2017).
- 19. M. N. Polyanskiy, Refractive index database.
- 20. D. M. Bigg, *Journal of Rheology*, **28**, 501 (1984).
- 21. S. A. Jenekhe and X. L. Chen, *Science*, **283**, 372 (1999).
- L. Vaisman, G. Marom, and H. D. Wagner, Advanced Functional Materials, 16, 357 (2006).
- D. Li, M. B. Müller, S. Gilje, R. B. Kaner, and G. G. Wallace, *Nature nanotechnology*, 3, 101 (2008).
- C. Selomulya, G. Bushell, R. Amal, and T. D. Waite, *Chemical Engineering Science*, 58, 327 (2003).
- 25. N. A. Mishchuk, Advances in Colloid and Interface Science, 168, 149 (2011).
- 26. H. J. Ploehn and W. B. Russel, Advances in Chemical Engineering, 15, 137 (1990).
- 27. P.-G. de Gennes, *Macromolecules*, 15, 492 (1982).
- 28. P.-G. de Gennes, Macromolecules, 14, 1637 (1981).
- 29. J. Klein and G. Rossi, Macromolecules, 31, 1979 (1998).
- 30. V. Runkana, P. Somasundaran, and P. C. Kapur, **61**, 182 (2006).
- 31. V. B. Derjaguin, Kolloid-Z, 69, 155 (1934).
- D. H. Napper, Polymeric stabilization of colloidal dispersions, Academic Press Incorporated (1983).
- J. H. Masliyah and S. Bhattacharjee, Electrokinetic and Colloid Transport Phenomena, Wiley (2006).
- M. Elimelech, J. Gregory, X. Jia, and R. Williams, *Particle deposition and aggregation*, p. 434 (1995).
- 35. R. Xu, Carbon, 45, 2806 (2007).
- 36. J. N. Israelachvili, Intermolecular and Surface Forces, 674 (2011).
- S. Ma, Q. Chen, F. H. Jøgensen, P. C. Stein, and E. M. Skou, *Solid State Ionics*, 178, 1568 (2007).
- E. B. Gutoff, E. D. Cohen, and G. I. Kheboian, Coating and Drying Defects Troubleshooting Operating Problems, 348 (2006).
- E. O. Machiste and G. Buckton, *International Journal of Pharmaceutics*, 145, 197 (1996)
- 40. K. S. Siow and D. Patterson, The Journal of Physical Chemistry, 77, 356 (1973).
- M. R. Somalu, A. Muchtar, W. Ramli, W. Daud, and N. P. Brandon, *Renewable and Sustainable Energy Reviews*, 75, 426 (2017).
- 42. T. F. Tadros, Rheology of Dispersions: Principles and Applications, (2010).
- P. Gallo, C. Cristiani, G. Dotelli, L. Omati, L. Zampori, R. Pelosato, and M. Guilizzoni, *Catalysis Today*, 147S, 30 (2009).
- 44. R. Durairaj, A. Seman, and N. N. Ekere, in, p. 347 (2006).
- D. C. Huang, P. J. Yu, F. J. Liu, S. L. Huang, K. L. Hsueh, Y. C. Chen, C. H. Wu, W. C. Chang, and F. H. Tsau, *International Journal of Electrochemical Science*, 6, 2551 (2011).